Hindawi Publishing Corporation
EURASIP Journal on Advances in Signal Processing
Volume 2010, Article ID 172751, 12 pages
doi:10.1155/2010/172751

Research Article

Optimized Paraunitary Filter Banks for Time-Frequency Channel Diagonalization

Ziyang Ju, Thomas Hunziker, and Dirk Dahlhaus

Communications Laboratory, University of Kassel, Wilhelmshöher Allee 73, 34121 Kassel, Germany

Correspondence should be addressed to Ziyang Ju, ju@uni-kassel.de

Received 17 June 2009; Revised 7 November 2009; Accepted 31 December 2009

Academic Editor: Faouzi Bader

We adopt the concept of channel diagonalization to time-frequency signal expansions obtained by DFT filter banks. As a generalization of the frequency domain channel representation used by conventional orthogonal frequency-division multiplexing receivers, the time-frequency domain channel diagonalization can be applied to time-variant channels and aperiodic signals. An inherent error in the case of doubly dispersive channels can be limited by choosing adequate windows underlying the filter banks. We derive a formula for the mean-squared sample error in the case of wide-sense stationary uncorrelated scattering (WSSUS) channels, which serves as objective function in the window optimization. Furthermore, an enhanced scheme for the parameterization of tight Gabor frames enables us to constrain the window in order to define paraunitary filter banks. We show that the design of windows optimized for WSSUS channels with known statistical properties can be formulated as a convex optimization problem. The performance of the resulting windows is investigated under different channel conditions, for different oversampling factors, and compared against the performance of alternative windows. Finally, a generic matched filter receiver incorporating the proposed channel diagonalization is discussed which may be essential for future reconfigurable radio systems.

1. Introduction

Motivated by the heterogeneity of today's world of wireless communications—which includes cellular mobile radio systems of the second and third generations and beyond, wireless local and personal area networks, broadband wireless access systems, digital audio and video broadcast, emerging peer-to-peer radio, and so forth—particular attention is given to reconfigurable radio architectures. Essential in this context are radio resource management solutions on the higher layers and the ability to comply with a range of different air interfaces on the physical layer. Devices comprising the logic for handling multiple air interfaces in the form of parallel implementations are widely available. However, in view of the still increasing number of standards, monolithic transceiver architectures are desirable which enable a uniform processing of different signals by means of reconfigurable multipurpose signal processing units.

A major challenge in the design of a universal baseband receiver architecture is posed by the dispersive radio channel. For dealing with signal dispersion, fundamentally different approaches are followed in traditional radios depending on the type of modulation. Receivers for single-carrier signals typically model the channel as a tapped delay line. For known coefficients of the delay line, the information in the transmitted signal can be recovered by means of a matched filtering followed by a sequence detector or using instead an equalizer followed by a simple detector. The complexity of the coefficient estimation and detection schemes increases with the delay dispersion and thus with the number of taps. Orthogonal frequency-division multiplexing (OFDM) can evade the need for complex equalizers in high data rate systems. The cyclic extensions in OFDM signals facilitate a frequency domain representation of the multipath channel in the form of parallel single-tap lines. On the basis of the frequency domain signal description resulting from the blockwise Discrete Fourier Transform (DFT), the signal mapping by multipath channels can be represented as diagonal matrices. This channel *diagonalization* enables straightforward demodulation and coefficient estimation and has, along with the availability of Fast Fourier Transform (FFT) algorithms, led to the popularity of OFDM.

The aforementioned approach for a simple channel inversion based on a frequency domain description is not limited to OFDM receivers. Single-carrier modulation with frequency domain equalization (FDE) can achieve similar performance as OFDM if a proper cyclic prefix is appended to each block of signals [1]. In [2] the computational complexities of time and frequency domain equalizers are compared and it is shown that FDE is simpler when the length of the stationary channel impulse response exceeds the sample time by a factor of 5 or more. Processing signals without cyclic prefix result in errors at the block boundaries. These errors have a limited impact at sufficiently large block sizes, which makes FDE an interesting alternative for code-division multiple access receivers [3, 4].

The limitations of OFDM receivers and FDE to time-invariant channels and certain signal formats can be overcome by resorting to alternative signal representations. A natural choice for the signal transform is the discrete-time Gabor expansion [5] based on a system of time-frequency (TF) shifted versions of a certain window function. Even though a TF domain channel diagonalization based on such a Gabor expansion is approximative in the general case of time-variant channels and aperiodic signals, for the typical underspread channels encountered in mobile radio scenarios the inherent model error can be limited to a usually acceptable level by choosing an adequate window underlying the signal transform [6].

The transform of discrete-time signals into the TF domain can be accomplished by DFT filter banks, for which similarly efficient FFT-based implementations are available as for plain DFTs [7]. There is plenty of literature on filter bank design in the context of generalized multicarrier/multitone modulation in wireless/wired communications. Replacing the block-wise inverse DFT and DFT in the transmitter and receiver, respectively, by more general filter banks is a way to get rid of the rigid framework of rectangular windows and cyclic prefixes in OFDM systems. Interference between adjacent sub-bands or multicarrier symbols can be avoided, or at least limited, by choosing appropriate transmit pulses. Filter banks for transmission over dispersive channels with limited interchannel and intersymbol interference are designed in [8–14].

The optimization of filter banks for specific objective functions and constraints can sometimes be formulated as a convex optimization (CO) problem [12]. In [15], CO methods are employed for the design of a two-channel multirate filter bank, in [16] for the design of pulse shapes which minimize intercarrier interference due to frequency offsets in OFDM systems, in [17] for finding optimized prototype filters for filtered multitone modulation used in digital subscriber line systems, and in [18] for the design of filter banks for sub-band signal processing under minimal aliasing and induced distortion. Semidefinite programming (SDP), a branch of CO for which efficient numerical solution methods are available, was employed in [19] for the design of a linear phase prototype filter with high stopband attenuation for cosine-modulated filter banks. In [20] two-channel filter banks are optimized under similar criteria by SDP.

In this paper we are not concerned with the design of transmit pulses. Rather, we optimize filter banks in the context of channel diagonalization. We are interested exclusively in paraunitary filter banks, which are related to the concept of tight Gabor frames [21]. The signal transform associated with discrete-time tight Gabor frames fulfills Parseval's identity. This property is crucial for flexible receivers as it lets the correlation between two time domain signals be computed based on the respective TF signal representations. A main concern of this paper is the design of tight Gabor frames facilitating TF domain channel diagonalization with minimal model error for given channel conditions. More specifically, we minimize the mean-squared error (MSE) resulting from the diagonalization of random channels with known second-order statistical properties, complying with the wide-sense stationary uncorrelated scattering (WSSUS) model, with respect to the TF window function. As we showed in [6], window functions minimizing the MSE appearing in the TF domain can be computed by SDP. In this paper we directly focus on the more relevant MSE in the time domain signal. We show that for weak assumptions on the channel statistics, the optimization problem can likewise be turned into a tractable form through semidefinite relaxation. In order to be able to constrain the windows to constitute tight frames, we extend the parameterization of tight Gabor frames presented in [22]. Optimized windows can then be computed off-line for different channel conditions encountered by reconfigurable receivers, such as the generic matched filter-based inner receiver discussed in this paper.

1.1. Outline of This Paper. In Section 2, the mathematical concepts for TF representation and processing of signals are introduced. A parameterization of tight Gabor frames, needed for the constrained optimization in Section 5 is presented in Section 3. In Section 4, TF domain channel diagonalization is discussed, resulting in a certain error in the case of doubly dispersive channels. As shown in Section 5, semidefinite relaxation lets the window design problem be formulated as a CO problem. Numerical results are shown in Section 6 for different channel conditions. In Section 7, a generic matched filter architecture incorporating the channel diagonalization is presented. Finally, conclusions are drawn in Section 8.

1.2. Notation. We enclose the arguments of functions defined on a discrete domain Λ in square brackets in order to distinguish them from functions defined on $\mathbb{R}^n$. The Hilbert space of the square summable functions $f : \Lambda \to \mathbb{C}$ is denoted as $L^2(\Lambda)$, and the associated inner product $\langle f, g\rangle$ and L^2-norm $\|f\|$ are given by $\sum_{i\in\Lambda} f[i]g^*[i]$ and $\sqrt{\langle f, f\rangle}$, respectively, where the asterisk in the superscript denotes complex conjugation. Furthermore, we use $*$ to denote convolution, and $\odot$ for the one-by-one multiplication of two compatible functions f and g, that is, $h = f \odot g$ corresponds to $h[i] = f[i]g[i]$ for all $i \in \Lambda$. Vectors and matrices are denoted by boldface characters. The transpose and Hermitian transpose of a matrix $\mathbf{X}$ are denoted as $\mathbf{X}^T$ and $\mathbf{X}^H$, respectively, $\widetilde{\mathbf{X}}(z)$ stands for the paraconjugate

of a polynomial matrix $\mathbf{X}(z)$ ($\widetilde{\mathbf{X}}(z)$ is obtained from $\mathbf{X}(z)$ by transposing it, conjugating all of the coefficients of the rational functions in $\mathbf{X}(z)$, and replacing z by z^{-1} [7].), $\mathrm{tr}(\cdot)$ for the trace, and $\mathbf{I}_N$ denotes the identity matrix of size N. The nth element of the mth row of a matrix $\mathbf{X}$ is represented as $[\mathbf{X}]_{m,n}$. Also, $E[\cdot]$ denotes the expected value, $\Re(\cdot)$ and $\Im(\cdot)$ represent the real and imaginary parts, respectively, of complex arguments, mod the modulo operation, $\jmath \triangleq \sqrt{-1}$, and $\lfloor x \rfloor \triangleq \max\{n \in \mathbb{Z} : \ n \leq x\}$.

2. DFT Filter Banks and Discrete-Time Gabor Frames

In this section, we introduce signal representation concepts needed subsequently. Some important properties of discrete-time Gabor frames are recapitulated with an emphasis on tight frames and the relationship to DFT filter banks. For more insight into Gabor analysis and filter bank theory the reader is referred to the rich literature, for instance [7, 23–26].

Let N and K be two positive integer constants and $\Lambda \triangleq \mathbb{Z} \times \{0, \ldots, K-1\}$. Given a window function $g \in L^2(\mathbb{Z})$, the set

$$\{g_{\ell,m}[k] : (\ell, m) \in \Lambda\} \tag{1}$$

with

$$g_{\ell,m}[k] \triangleq g[k - \ell N] \exp\left(\frac{\jmath 2\pi(k - \ell N)m}{K}\right) \tag{2}$$

is referred to as a *Gabor system* in $L^2(\mathbb{Z})$. The elements of the Gabor system can be associated with the grid points $\{(\ell N, 2\pi m/K) : (\ell, m) \in \Lambda\}$ of a lattice overlaying the TF plane $\mathbb{Z} \times [0, 2\pi)$. If there exist two positive constants A_0 and B_0 such that

$$A_0\|x\|^2 \leq \sum_{(\ell,m)\in\Lambda} |\langle x, g_{\ell,m}\rangle|^2 \leq B_0\|x\|^2 \quad \forall x \in L^2(\mathbb{Z}), \tag{3}$$

then (1) represents a discrete-time *Gabor frame*. A necessary condition for (3) is that $N/K \leq 1$.

For an arbitrary signal $x \in L^2(\mathbb{Z})$ the inner products of $x[k]$ with every element of the system (1) form a linear TF representation. In the following, the corresponding transform onto $L^2(\Lambda)$ is represented by the analysis operator

$$\mathcal{G} : x \longmapsto X, \qquad X[\ell, m] = \langle x, g_{\ell,m}\rangle, \quad (\ell, m) \in \Lambda. \tag{4}$$

The mapping (4) can be implemented by a K-channel DFT (analysis) filter bank with a prototype filter with impulse response $g^*[-k]$ followed by a down-sampling by a factor N [21]. Conversely, a synthesis operator $\mathcal{G}^*$ can be defined based on (1) which maps an arbitrary TF representation $Y \in L^2(\Lambda)$ onto an element of $L^2(\mathbb{Z})$ according to

$$\mathcal{G}^* : Y \longmapsto \sum_{(\ell,m)\in\Lambda} Y[\ell, m] g_{\ell,m}[k]. \tag{5}$$

The signal synthesis (5) can be implemented by an up-sampling by a factor N followed by a K-channel DFT (synthesis) filter bank with a prototype filter with impulse response $g[k]$.

If (3) holds with $A_0 = B_0 = 1$ then (1) represents a (normalized) *tight* Gabor frame and $\mathcal{G}^*(\mathcal{G}x) = x$ for all $x \in L^2(\mathbb{Z})$. These special Gabor frames obey a generalized Parseval's identity

$$\|x\|^2 = \|\mathcal{G}x\|^2 \quad \forall x \in L^2(\mathbb{Z}). \tag{6}$$

Furthermore, the inner product $\langle x, y\rangle$ of any two $x, y \in L^2(\mathbb{Z})$ can be computed on the basis of the respective TF representations $\mathcal{G}x$ and $\mathcal{G}y$, that is,

$$\langle x, y\rangle = \langle \mathcal{G}x, \mathcal{G}y\rangle \quad \forall x, y \in L^2(\mathbb{Z}). \tag{7}$$

Henceforth we assume that (1) represents a tight Gabor frame. We note that the range $\mathcal{F}_g \triangleq \{(\mathcal{G}x)[k] : x \in L^2(\mathbb{Z})\}$ of the operator $\mathcal{G}$ is a subspace of $L^2(\Lambda)$, and the mapping $\mathcal{G} : L^2(\mathbb{Z}) \to \mathcal{F}_g$ is an isometry. If $N/K < 1$ the operator $\mathcal{G}\mathcal{G}^*$ represents the orthogonal projection from $L^2(\Lambda)$ onto $\mathcal{F}_g$. As a direct consequence,

$$\|\mathcal{G}^*X\|^2 \leq \|X\|^2 \quad \forall X \in L^2(\Lambda) \tag{8}$$

and $\|g\|^2 = N/K$.

Tight Gabor frames are associated with *paraunitary* DFT filter banks. To enable the design of windows with favorable properties, for instance in regard to TF concentration, it is often necessary to indeed choose $N < K$, resulting in *oversampled* filter banks. Besides of available efficient implementations of paraunitary DFT filter banks, the properties (6) and (7) are of prime interest for reconfigurable baseband receivers since they allow operations for the signal demodulation, such as signal energy computations and crosscorrelations with reference waveforms, to be performed directly in the TF domain.

3. Parameterization of Tight Gabor Frames

The conditions under which (1) represents a tight Gabor frame can be formulated via the polyphase representation. Let M denote the least common multiple of N and K, and define L and J such that $LN = M$ and $JK = M$. The M-component polyphase representation of the z-transform $G(z) = \sum_{k=-\infty}^{\infty} g[k]z^{-k}$ of the window $g[k]$ reads

$$G(z) = \sum_{j=0}^{M-1} z^{-j} R_j\left(z^M\right), \tag{9}$$

where

$$R_j(z) = \sum_{k\in\mathbb{Z}} g[j + kM]z^{-k}. \tag{10}$$

Furthermore, the polyphase matrix $\mathbf{G}_{\mathrm{P}}(z)$ of size $K \times N$ associated with the DFT filter bank implementing (4) can be expressed as [22]

$$\mathbf{G}_{\mathrm{P}}(z) = \mathbf{F}_K \mathbf{V}(z) \tag{11}$$

with $\mathbf{F}_K$ denoting the DFT matrix of size K (defined as $[\mathbf{F}_K]_{m,n} = e^{-\jmath 2\pi(m-1)(n-1)/K}$) and

$$\mathbf{V}(z) \triangleq \left[\underbrace{\mathbf{I}_K \cdots \mathbf{I}_K}_{J}\right] \operatorname{diag}\left(R_0\left(z^L\right), \ldots, R_{M-1}\left(z^L\right)\right) \begin{bmatrix} \mathbf{I}_N \\ z^{-1}\mathbf{I}_N \\ \vdots \\ z^{-(L-1)}\mathbf{I}_N \end{bmatrix}. \tag{12}$$

Here, $\operatorname{diag}(d_1, \ldots, d_N)$ is the diagonal matrix with diagonal elements $d_1, \ldots, d_N$. The Gabor system (1) represents a tight frame in $L^2(\mathbb{Z})$ if and only if the polyphase matrix $\mathbf{G}_{\mathrm{P}}(z)$ is paraunitary with $\widetilde{\mathbf{G}}_{\mathrm{P}}(z)\mathbf{G}_{\mathrm{P}}(z) = \mathbf{I}_N$. Or, equivalently, if and only if the polynomial matrix $\mathbf{V}(z)$ is paraunitary with $\widetilde{\mathbf{V}}(z)\mathbf{V}(z) = K^{-1}\mathbf{I}_N$, since $\mathbf{F}_K^H\mathbf{F}_K = K\mathbf{I}_K$.

We observe that $[\mathbf{V}(z)]_{m,n} = 0$ if $((m-n) \bmod B) \neq 0$, where $B = N/J = K/L$. Consequently, $\mathbf{V}(z)$ is paraunitary if and only if the B matrices $\mathbf{V}_0(z), \ldots, \mathbf{V}_{B-1}(z)$ of size $L \times J$, which comprise the possibly nonzero elements of $\mathbf{V}(z)$ according to $[\mathbf{V}_b(z)]_{m,n} = [\mathbf{V}(z)]_{1+B(m-1)+b,1+B(n-1)+b}$, are all paraunitary. As follows from (12) the elements of the B matrices are given as

$$[\mathbf{V}_b(z)]_{m,n} = z^{-\lfloor f(m,n)/J \rfloor} R_{Bf(m,n)+b}\left(z^L\right), \quad b = 0, \ldots, B-1 \tag{13}$$

with $f(m,n) \triangleq \sum_{j=0}^{J-1}\sum_{\ell=0}^{L-1}(m + jL - 1)\delta_{m+jL,n+\ell J}$ and $\delta_{i,j}$ denoting the Kronecker delta.

Note that if the sequences $(\lfloor f(m,n)/J \rfloor)_{m=1,\ldots,L}$ were identical for all column indices $n = 1, \ldots, J$ except for differing offsets, then the factor $z^{-\lfloor f(m,n)/J \rfloor}$ could be omitted in (13) without affecting the condition $\widetilde{\mathbf{V}}_b(z)\mathbf{V}_b(z) = K^{-1}\mathbf{I}_J$. Replacing some $R_m(z^L)$ by the equivalent $z^{-L}R_{M+m}(z^L)$ is a way to align the sequences. Having this in mind, we define B matrices $\mathbf{W}_0(z), \ldots, \mathbf{W}_{B-1}(z)$ of size $L \times J$ according to

$$[\mathbf{W}_b(z)]_{m,n} = R_{Bf'(m,n)+b}(z), \quad b = 0, \ldots, B-1 \tag{14}$$

with the index map

$$f'(m,n) \triangleq \begin{cases} f(m,n) & \text{if } f(m,n) \geq f(1,n) \\ f(m,n) + \dfrac{M}{B} & \text{if } f(m,n) < f(1,n). \end{cases} \tag{15}$$

Since the polynomial matrices $\mathbf{V}_0(z), \ldots, \mathbf{V}_{B-1}(z)$ are paraunitary if and only if the modified matrices $\mathbf{W}_0(z), \ldots, \mathbf{W}_{B-1}(z)$ are paraunitary, the Gabor system (1) represents a tight frame in $L^2(\mathbb{Z})$ if and only if

$$\widetilde{\mathbf{W}}_b(z)\mathbf{W}_b(z) = K^{-1}\mathbf{I}_J \quad \forall b \in \{0, \ldots, B-1\}. \tag{16}$$

We note that the size of each polynomial matrix $\mathbf{W}_b(z)$, their number B, and the index map $f'(m,n)$ are fully determined by N and K. Given the latter two constants, any tight Gabor frame is uniquely defined by an instance of $\mathbf{W}_0(z), \ldots, \mathbf{W}_{B-1}(z)$ satisfying (16), where the association of the elements of the B matrices with the samples of the window $g[k]$ is defined by (14) and (10). The length of the window is related to the polynomial orders of the matrices $\mathbf{W}_0(z), \ldots, \mathbf{W}_{B-1}(z)$. We define P as the maximal polynomial order of the B matrices plus 1. Thus, in the case $P = 1$, all elements of the matrices are scalars, and the support of the representable functions $g[k]$ is limited to $\{Bf'(m,n) + b : m = 1, \ldots, L; n = 1, \ldots, J; b = 0, \ldots, B-1\}$. This set is usually not of the form $\mathbb{Z} \cap [a_0, b_0]$ for some $a_0 \leq b_0$ but exhibits "gaps" as illustrated in the example of Figure 1. By increasing P longer windows can be found.

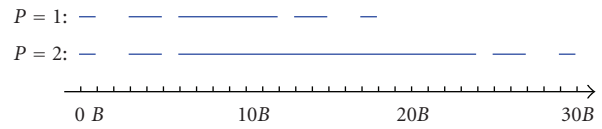

Figure 1: Support of the window functions $g[k]$ representable by matrices $\mathbf{W}_0(z), \ldots, \mathbf{W}_{B-1}(z)$ with maximal polynomial order $P-1$ for $J = 3$, $L = 4$, $P = 1, 2$.

4. Time-Frequency Channel Diagonalization

The mapping $\mathcal{H} : L^2(\mathbb{Z}) \to L^2(\mathbb{Z})$ of an input signal $x[k]$ onto the signal $y[k] \triangleq (\mathcal{H}x)[k]$ at the output of a linear time-variant channel can be expressed as

$$y[k] = \sum_{q=0}^{\infty} c_{\mathcal{H}}[k,q]x[k-q], \tag{17}$$

where $c_{\mathcal{H}}[k,q]$ denotes the time-variant impulse response. We consider random channels where $c_{\mathcal{H}}[k,q]$ represents a two-dimensional zero-mean random process complying with the WSSUS model. The second-order statistics of $c_{\mathcal{H}}[k,q]$ are determined by the time correlation function $\phi_t[k_\Delta]$ and the delay power spectrum $S_{\text{delay}}[q]$ according to

$$E[c_{\mathcal{H}}[k,q]c^*_{\mathcal{H}}[k',q']] = \phi_t[k-k']S_{\text{delay}}[q]\delta_{q,q'}. \tag{18}$$

The delay power spectrum is related to the frequency correlation function $\phi_f(\omega_\Delta)$ through

$$\phi_f(\omega_\Delta) = \sum_{q=0}^{\infty} S_{\text{delay}}[q]e^{-\jmath\omega_\Delta q}. \tag{19}$$

Of interest in the context of TF signal processing is the time-variant transfer function

$$C_{\mathcal{H}}(k,\omega) = \sum_{q=0}^{\infty} c_{\mathcal{H}}[k,q]e^{-\jmath\omega q}, \tag{20}$$

reflecting the TF selectivity of a channel realization. In a digital receiver a realization of a doubly dispersive channel can be represented by a sampled version $H[\ell,m]$ of $C_{\mathcal{H}}(k,\omega)$, defined by

$$H[\ell,m] = C_{\mathcal{H}}\left(\ell N, \frac{2\pi m}{K}\right), \quad (\ell,m) \in \Lambda. \tag{21}$$

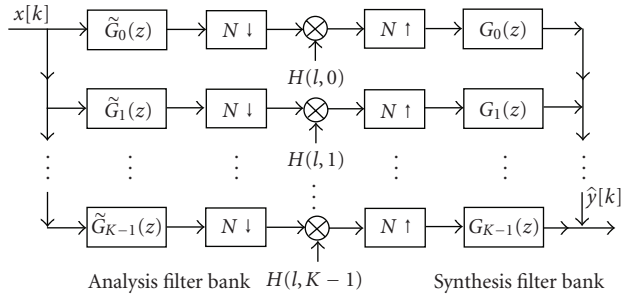

FIGURE 2: TF domain channel diagonalization with $G_k(z) \triangleq G(ze^{\jmath 2\pi k/K})$, $k = 0, \ldots, K-1$.

For compatibility with the TF signal representations introduced in Section 2, the sampling intervals N and $2\pi/K$ are chosen in line with those for the Gabor system (1). The time-variant transfer function represents the complex-valued channel gain over time and frequency. Hence, given the TF representation $X \triangleq \mathcal{G}x$ of a signal $x[k]$ at the channel input, it is straightforward to approximate the signal $y[k]$ at the channel output as

$$\hat{y} = \mathcal{G}^*(H \odot X). \tag{22}$$

The approximation of a linear operator by $\mathcal{G}^*(H \odot \mathcal{G}(\cdot))$, that is, a concatenation of an analysis operation, an element-wise multiplication, and a synthesis operation, appears in the literature under the name *Gabor multiplier* [27]. Such an approximation is suitable for operators that do not involve TF shifts of large magnitude (i.e., underspread operators). Figure 2 shows an implementation of (22) by filter banks, where $G(z)$ denotes the z-transform of $g[k]$. The TF channel diagonalization offers several advantages. The flexibility in the choice of the sampling intervals N and $2\pi/K$ can be used for the adaptation to different channel conditions or signal formats, or the limitation of the effort for the coefficient estimation in certain receivers. Furthermore, the channel diagonalization facilitates scalable and efficient receiver processing known from OFDM.

As a result of the sampling of $C_{\mathcal{H}}(k, \omega)$ the model (22) is usually only approximative, and $\hat{y}[k]$ is an approximation of the channel output. The accuracy of $\hat{y}[k]$ depends on the channel characteristics and the underlying Gabor frame. We may expect the model error to be limited if every elementary function $g_{\ell,m}[k]$ is concentrated around $(\ell N, 2\pi m/K)$ in the TF plane such that $C_{\mathcal{H}}(k, \omega)$ is essentially constant within the sphere of $g_{\ell,m}[k]$. Window functions fulfilling this can be designed for the typical underspread channels encountered in mobile radio scenarios by CO, as shown in Section 5.

The error from the channel diagonalization is given by

$$\hat{y}[k] - y[k] = (\mathcal{G}^*(H \odot \mathcal{G}x))[k] - (\mathcal{H}x)[k]. \tag{23}$$

In order to remain general in regard to signal and channel properties, we consider the error signal under the assumptions of

(i) a white random signal at the channel input,

(ii) a random channel $\mathcal{H}$ complying with the WSSUS model and unit average channel gain (i.e., $\phi_f(0) = \phi_t[0] = 1$).

To formulate the resulting MSE, we introduce the random signal $x_Q[k]$ being subject to $E[x_Q[k]] = 0$ and

$$E\left[x_Q^*[k]x_Q[k']\right] = \begin{cases} \delta_{k,k'} & \text{for } k, k' \in \left[-\frac{Q}{2}, \frac{Q}{2}\right] \\ 0 & \text{otherwise} \end{cases} \tag{24}$$

with Q an even integer. The error signal corresponding to the truncated white random input signal $x_Q[k]$ reads

$$\epsilon_Q[k] \triangleq (\mathcal{G}^*(H \odot \mathcal{G}x_Q))[k] - (\mathcal{H}x_Q)[k]. \tag{25}$$

The error signal sample energy relative to the unit average sample energy of the desired signal, in the following termed relative mean-squared sample error (RMSSE), can be expressed as

$$\begin{aligned} \varepsilon_{\text{RMSSE}}(g) &= \lim_{Q\to\infty} E\left[\frac{1}{Q}\sum_{k=-Q/2}^{Q/2} |\epsilon_Q[k]|^2\right] \\ &= \lim_{Q\to\infty} E\left[\frac{1}{Q}\sum_{k=-Q/2}^{Q/2}\left|\sum_{(\ell,m)\in\Lambda} H[\ell,m]\langle x_Q, g_{\ell,m}\rangle \times g_{\ell,m}[k] - (\mathcal{H}x_Q)[k]\right|^2\right]. \end{aligned} \tag{26}$$

Making use of the above assumptions, the RMSSE can be written as

$$\varepsilon_{\text{RMSSE}}(g) = 1 + \frac{K}{N}\left(\sum_{(\ell,m)\in\Lambda}\phi_t[\ell N]\phi_f\left(\frac{2\pi m}{K}\right)|\langle g, g_{\ell,m}\rangle|^2 - 2\Re\left(\left\langle\left(g * S_{\text{delay}}\right)\odot\phi_t, g\right\rangle\right)\right) \tag{27}$$

as shown in the appendix. Having formulated both conditions for the window $g[k]$ to define a tight Gabor frame (in Section 3) and the error resulting from the channel diagonalization based on $g[k]$, we can now turn to window optimization.

5. Window Design

Let us represent the window to be optimized in vector form $\mathbf{g} \triangleq [g[a_0] \cdots g[b_0]]^{\mathrm{T}}$, choosing $a_0, b_0 \in \mathbb{Z}$ such that $[a_0, b_0]$ comprises the support of $g[k]$ expressed in Section 3. We consider only real-valued windows. Additionally, in order to eventually arrive at a CO problem, we impose the following restrictions on the channel statistics.

(i) The time correlation function is subject to $\phi_t[\ell] \geq 0$ for all $\ell \in \mathbb{Z}$, as being the case for two-sided exponentially decaying and many other symmetrical Doppler power spectra.

(ii) The frequency correlation function fulfills $\phi_f(2\pi m/K) + \phi_f(-2\pi m/K) \geq 0$ for all $m \in \{0,\ldots,K-1\}$, as, for instance, in the case of exponentially decaying delay power spectra.

We note that $|\langle g, g_{\ell,m}\rangle|^2$ can be expressed as $(\mathbf{g}^T\Re(\mathbf{C}_{\ell,m})\mathbf{g})^2 + (\mathbf{g}^T\Im(\mathbf{C}_{\ell,m})\mathbf{g})^2$ and $\Re(\langle(g * S_{\text{delay}}) \odot \phi_t, g\rangle)$ as $\mathbf{g}^T\Re(\mathbf{D}_0)\mathbf{g}$ with appropriate square matrices $\mathbf{C}_{\ell,m}$ and $\mathbf{D}_0$. As a consequence, the objective function (27) can be expressed in the form

$$\varepsilon_{\text{RMSSE}}(\mathbf{g}) = \sum_{k=1}^{F} c_k\left(\mathbf{g}^T\mathbf{C}_k\mathbf{g}\right)^2 + \mathbf{g}^T\mathbf{D}\mathbf{g} + 1 \tag{28}$$

for some $F \in \mathbb{N}$ depending on the support of $g[k]$, where $\mathbf{C}_1,\ldots,\mathbf{C}_F,\mathbf{D}$ are real matrices and the constants $c_1,\ldots,c_F$ are positive given the above restrictions.

Next, we need to incorporate the constraints under which $\varepsilon_{\text{RMSSE}}(\mathbf{g})$ will be minimized. In order to formulate the constraints (16) on the window in the time domain, it is helpful to permute the samples in $\mathbf{g}$. Let us introduce a window $(h[0],\ldots,h[T-1])$ of length $T = LJPB$ defined as

$$h[k] = g[Bf'(m,n) + b + Mp], \quad k = 0,\ldots,T-1 \tag{29}$$

with $m = (k \bmod L) + 1$, $n = \lfloor (k \bmod LJ)/L \rfloor + 1$, $p = \lfloor (k \bmod LJP)/(LJ) \rfloor$, and $b = \lfloor k/(LJP) \rfloor$. The matrices $\mathbf{W}_0(z),\ldots,\mathbf{W}_{B-1}(z)$ and the samples of the permuted window are related through

$$[\mathbf{W}_b(z)]_{m,n} = \sum_{p=0}^{P-1} h[L(J(bP+p)+n-1)+m-1]z^{-p}. \tag{30}$$

With (30) we can now translate the polyphase domain constraints (16) into constraints on the permuted window defined by $\mathbf{h} \triangleq [h[0]\cdots h[T-1]]^T$.

(1) Case $B = 1$. There are J constraints of form $\mathbf{h}^T\mathbf{A}_\ell\mathbf{h} = K^{-1}$. The ℓth diagonal matrix $\mathbf{A}_\ell$ of size $LJP \times LJP$ is defined as

$$[\mathbf{A}_\ell]_{m,n} = \begin{cases} 1 & \text{if } m = n, \\ & m \in \bigcup_{p=0,\ldots,P-1} \{(pJ+\ell-1)L+1, \\ & \qquad \ldots, (pJ+\ell)L\}, \\ 0 & \text{otherwise,} \end{cases} \tag{31}$$

with $\ell \in \{1,\ldots,J\}$. Additionally, there are $J^2P - (J+1)J/2$ constraints of form $\mathbf{h}^T\mathbf{A}_\ell\mathbf{h} = 0$. The corresponding matrices $\mathbf{A}_{J+1},\ldots,\mathbf{A}_{J^2P-(J-1)J/2}$ can be defined as the elements of the set resulting from deleting duplicate elements and zero-matrices from

$$\Big\{\mathbf{A} \in \mathbb{R}^{LJP\times LJP} \text{ given as } [\mathbf{A}]_{m,n} = [\mathbf{A}_\ell]_{m-jL,n} + [\mathbf{A}_\ell]_{m,n-jL} : j = 1,\ldots,JP; \ell = 1,\ldots,J\Big\} \tag{32}$$

where in (32) we let $[\mathbf{A}_\ell]_{m,n}$ equal zero if either $m \notin \{1,\ldots,LJP\}$ or $n \notin \{1,\ldots,LJP\}$.

(2) Case $B > 1$. From each of the above-defined matrices $\mathbf{A}_1,\ldots,\mathbf{A}_{J^2P-(J-1)J/2}$, B unique block diagonal matrices of dimension $T \times T$ are reproduced which contain the original matrix as one of the B diagonal blocks of dimension $LJP \times LJP$. Hence, there are $W \triangleq B(J^2P - (J-1)J/2)$ constraints in total. The constraint matrices are mutually orthogonal in the sense that $\operatorname{tr}(\mathbf{A}_\ell\mathbf{A}_m^T) = 0$ for $\ell \neq m$.

We can now formulate the optimization problem in the form

$$\begin{aligned} &\min_{\mathbf{h}\in\mathbb{R}^T} \sum_{k=1}^{F} c_k\left(\mathbf{h}^T\hat{\mathbf{C}}_k\mathbf{h}\right)^2 + \mathbf{h}^T\hat{\mathbf{D}}\mathbf{h} \\ &\text{subject to } \mathbf{h}^T\mathbf{A}_\ell\mathbf{h} = d_\ell, \quad \ell = 1,\ldots,W, \end{aligned} \tag{33}$$

where $\hat{\mathbf{C}}_1,\ldots,\hat{\mathbf{C}}_F,\hat{\mathbf{D}}$ are the matrices resulting from $\mathbf{C}_1,\ldots,\mathbf{C}_F,\mathbf{D}$ by permuting the rows and columns in accordance with (29), and $d_\ell \in \{K^{-1},0\}$. This problem is difficult to tackle for large T. Let us thus introduce $\mathbf{H} \triangleq \mathbf{h}\mathbf{h}^T$ and reformulate the optimization problem as

$$\begin{aligned} &\min_{\mathbf{H}\in\mathcal{S}_T} \sum_{k=1}^{F} c_k \operatorname{tr}^2\left(\mathbf{H}\hat{\mathbf{C}}_k\right) + \operatorname{tr}\left(\mathbf{H}\hat{\mathbf{D}}\right) \\ &\text{subject to } \begin{cases} \operatorname{tr}(\mathbf{H}\mathbf{A}_\ell) = d_\ell, & \ell = 1,\ldots,W \\ \operatorname{rank}(\mathbf{H}) = 1, \end{cases} \end{aligned} \tag{34}$$

where $\mathcal{S}_T$ denotes the vector space of symmetric matrices of dimension $T \times T$. In (34) we have a convex objective function, however, the set $\{\mathbf{H} \in \mathcal{S}_T : \operatorname{rank}(\mathbf{H}) = 1\}$ is nonconvex. Resorting to semidefinite relaxation, we obtain

$$\begin{aligned} &\min_{\mathbf{H}\in\mathcal{S}_T} \sum_{k=1}^{F} c_k \operatorname{tr}^2\left(\mathbf{H}\hat{\mathbf{C}}_k\right) + \operatorname{tr}\left(\mathbf{H}\hat{\mathbf{D}}\right) \\ &\text{subject to } \begin{cases} \operatorname{tr}(\mathbf{H}\mathbf{A}_\ell) = d_\ell, & \ell = 1,\ldots,W \\ \mathbf{H} \succeq 0 \end{cases} \end{aligned} \tag{35}$$

with $\mathbf{H} \succeq 0$ denoting that $\mathbf{H}$ is positive semidefinite. Since $\{\mathbf{H} \in \mathcal{S}_T : \mathbf{H} \succeq 0\}$ is a convex subset of $\mathcal{S}_T$, we now have a CO problem [28]. Having found a matrix $\mathbf{H}_0 \in \mathcal{S}_T$ corresponding to a global minimum of (35), we have two possible cases. If $\operatorname{rank}(\mathbf{H}_0) = 1$, a solution $\mathbf{h}_0$ of (33) is readily obtainable from $\mathbf{h}_0\mathbf{h}_0^T = \mathbf{H}_0$ and the optimal window $g_{\text{CO}}[k]$ is found through (29). If $\operatorname{rank}(\mathbf{H}_0) > 1$, which we observe in most of the cases, rank reduction methods must be employed. We compute a possibly suboptimal window $g_{\text{CO}}[k]$ by the following three steps.

(i) In order to reduce the rank to 1, we resort to the matrix $\hat{\mathbf{H}}_0 = (N/K)\mathbf{v}_0\mathbf{v}_0^H$ composed by the dominant eigenvector $\mathbf{v}_0$ of $\mathbf{H}_0$, since $\hat{\mathbf{H}}_0$ is the matrix nearest to $\mathbf{H}_0$ in terms of the Frobenius norm [29].

(ii) We translate $\sqrt{N/K}\mathbf{v}_0$ into a window $\hat{g}[k]$ taking the sample permutation defined in (29) into account.

(iii) We finally obtain $g_{\text{CO}}[k]$ by the algorithm [30], which yields a window defining a tight frame and at the

same time minimizes the distance to a given window (i.e., $\hat{g}[k]$) in terms of the L^2-norm.

Employing steepest descent methods for solving (35) may result in very slow convergence, whereas alternative methods may not be applicable when the number of dimensions is large. Neglecting the quadratic terms in the objective function leads to the simplified optimization problem

$$\min_{\mathbf{H}\in\mathcal{S}_T} \operatorname{tr}\left(\mathbf{H}\hat{\mathbf{D}}\right) \quad \text{subject to} \begin{cases} \operatorname{tr}(\mathbf{H}\mathbf{A}_\ell) = d_\ell, & \ell = 1,\ldots,W \\ \mathbf{H} \succeq 0. \end{cases} \tag{36}$$

As shown in [6], the linear objective function $\operatorname{tr}(\mathbf{H}\hat{\mathbf{D}})$ reflects the mean-squared deviation of $H \odot \mathcal{G}x$ from $\mathcal{G}(\mathcal{H}x)$, that is, the model error in the TF domain. Problems of the form (36) are dealt with by SDP, a subfield of CO. For the efficient solution of these optimization problems a number of sophisticated software packages are widely available. However, because generally $(H \odot \mathcal{G}x - \mathcal{G}(\mathcal{H}x)) \notin \mathcal{F}_g$ the windows resulting from solving (36) do not minimize the time domain error signal, the magnitude of which determines the performance of the channel diagonalization.

6. Numerical Results

We consider a WSSUS channel with an exponentially decaying delay power spectrum, the sampled version of which reads

$$S_{\text{delay}}[q] = u(q)\left(1 - \exp\left(-\frac{1}{\tau_{\text{RMS}}}\right)\right)\exp\left(-\frac{q}{\tau_{\text{RMS}}}\right) \tag{37}$$

with $u(q)$ denoting the unit step function and τ_{RMS} the root mean-squared (RMS) delay spread [31]. As for the Doppler power spectrum, a two-sided exponentially decaying shape is assumed, which results in the time correlation function

$$\phi_t[k_\Delta] = \frac{1}{1 + 2\pi^2\nu_{\text{RMS}}^2|k_\Delta|^2}, \tag{38}$$

where ν_{RMS} represents the RMS Doppler spread. Since choosing an oversampling factor K/N larger than one increases the degrees of freedom in the window design, we restrict our attention to scenarios with $K > N$, involving oversampled filter banks. Figure 3 shows optimized window functions for different channel conditions and their Fourier transforms. The waveforms were obtained numerically by solving (35) using interior point methods [28] for $N = 24$, $K = 32$, $P = 2$ amounting to a window length of 240 samples. An RMS delay spread τ_{RMS} of 3 samples and an RMS Doppler spread ν_{RMS} of 0.001 samples^{-1} were assumed in Figure 3(a), while $\tau_{\text{RMS}} = 3$, $\nu_{\text{RMS}} = 0.01$ in Figure 3(b). The two shown optimized windows achieve RMSSEs (27) of -16.01 dB and -8.44 dB. Figures 3(c) and 3(d) show the Fourier transforms of the optimized pulses in (a) and (b), respectively, versus the normalized frequency $\omega/2\pi$. Obviously, the optimized waveforms become more concentrated in time domain as the Doppler spread increases (see Figure 3(b) versus Figure 3(a)). For increasing Doppler spreads the coherence time of the channel decreases, and the temporal support of the optimized window is reduced in order to limit the RMSSE.

The RMSSEs (27) achievable by optimized windows are shown in Figure 4 for the same lattice constants and similar types of delay/Doppler power spectra. The RMS delay spread τ_{RMS} ranges between 0.5 and 8 samples while the RMS Doppler spread ν_{RMS} equals 0.01 samples^{-1}. For every considered τ_{RMS} a window $g_{\text{CO}}[k]$ was obtained by numerically solving the CO problem (35), and a window $g_{\text{SDP}}[k]$ by solving (36) through SDP, where both approaches required the above-mentioned additional steps for rank reduction. The global minimum of the objective function in (35) at $\mathbf{H} = \mathbf{H}_0$, that is prior to the rank reduction, serves as a lower bound in the figure. The offsets of $\varepsilon_{\text{RMSSE}}(g_{\text{CO}})$ and $\varepsilon_{\text{RMSSE}}(g_{\text{SDP}})$ from the lower bound reflect the impact of the rank reduction. Additionally, the figure shows the RMSSEs resulting from choosing a window $g_{\text{RRC}}[k]$ with a root-raised-cosine (RRC) shaped magnitude spectrum with width $2\pi/K$ and roll-off factor $K/N - 1$. We choose this window function for comparison because it does constitute a tight Gabor frame while exhibiting superior TF localization properties compared to rectangularly shaped windows for instance. Finally, for the verification of $\varepsilon_{\text{RMSSE}}(g_{\text{CO}})$ the signals $y = \mathcal{H}x$ and $\hat{y} = \mathcal{G}^*(H \odot (\mathcal{G}x))$ were also obtained by simulations involving filter banks based on the optimized windows $g_{\text{CO}}[k]$ and random signal and WSSUS channel generators, and the resulting error signal analyzed.

Obviously, solving (35) leads to better windows than solving (36). The considerable offset of the RMSSEs from the lower bound for smaller τ_{RMS} indicates that here the rank reduction has a significant impact on the windows. We observe that rank reduction generally has a limited effect when the delay and Doppler spreads are of similar extent, that is, when in the TF plane the delay spread relative to the sampling interval in time (i.e., τ_{RMS}/N) is of the same order of magnitude as the Doppler spread relative to the sampling interval in frequency (i.e., ν_{RMS}/K^{-1}).

The relatively high RMSSEs found in Figure 4 are a result of the product $\tau_{\text{RMS}}\nu_{\text{RMS}}$ being in the order of 10^{-2}, a much larger value than encountered in typical mobile radio scenarios. In environments with such severe dispersion in both time and frequency, the model error performance can actually be improved by increasing the oversampling factor K/N. This can be seen in Table 1, showing some $\varepsilon_{\text{RMSSE}}(g_{\text{CO}})$ observed under the same conditions as above except for choosing different lattice constants. An RMS delay spread of 1 sample is assumed here. The performance clearly improves with the oversampling factor.

7. Generic Matched Filter Receiver

The considered TF channel diagonalization does not rely on a particular signal format, making it suitable for application in multimode receivers [32]. The burst structures defined in the various standards for wireless communications differ

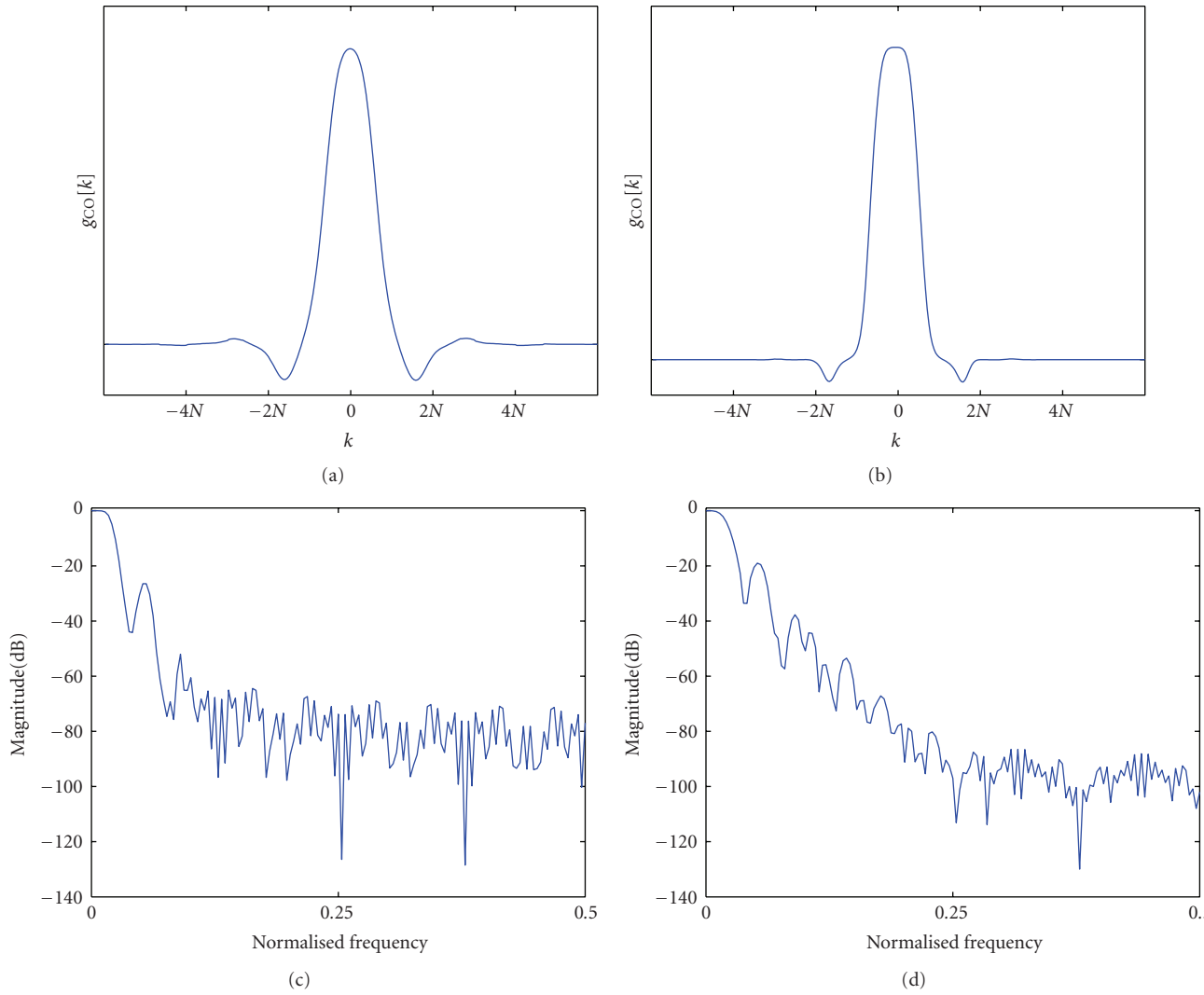

Figure 3: Examples of optimized window functions in time domain ((a) and (b)) and in frequency domain ((c) and (d)) for different channel statistics: $\tau_{\mathrm{RMS}} = 3$, $\nu_{\mathrm{RMS}} = 0.001$ (in (a) and (c)), $\tau_{\mathrm{RMS}} = 3$, $\nu_{\mathrm{RMS}} = 0.01$ (in (b) and (d)).

Table 1: Model error for different oversampling factors.

N	K	Oversampling factor	$\varepsilon_{\mathrm{RMSSE}}(g_{\mathrm{CO}})$
24	32	4/3	−9.49 dB
20	32	8/5	−11.78 dB
16	32	2	−14.83 dB
12	32	8/3	−18.57 dB
8	32	4	−22.43 dB
4	32	8	−23.25 dB

substantially. However, commonly the bursts incorporate preamble signals for the channel estimation along with information-bearing signals which are usually subject to a linear modulation scheme. The transmitted baseband signals generally follow the form $t[k] = \sum_{i=1}^{I} s_i z_i[k]$ with $z_1[k], \ldots, z_I[k]$ representing I elementary waveforms, possibly complex exponentials such as in the case of OFDM, or pseudo-noise sequences as in the case of direct-sequence spread-spectrum systems. For performing channel estimation and information recovery the receiver needs to estimate the signals $s_1, \ldots, s_I$ on the basis of the known waveforms $z_1[k], \ldots, z_I[k]$. To this end, the inner receiver correlates the received signal $r[k]$ with the elementary signals as appearing at the channel output, resulting in

$$u_i = \langle r, \mathcal{H} z_i \rangle, \quad i = 1, \ldots, I. \tag{39}$$

For example, in the case of signal decoding in the presence of additive white Gaussian noise, $u_1, \ldots, u_I$ represent a sufficient statistic. In other situations, such as for the channel parameter estimation (Efficient parameter estimators which are applicable in the context of filter bank-based multicarrier transmission are presented in [33].), $\mathcal{H}$ is unknown.

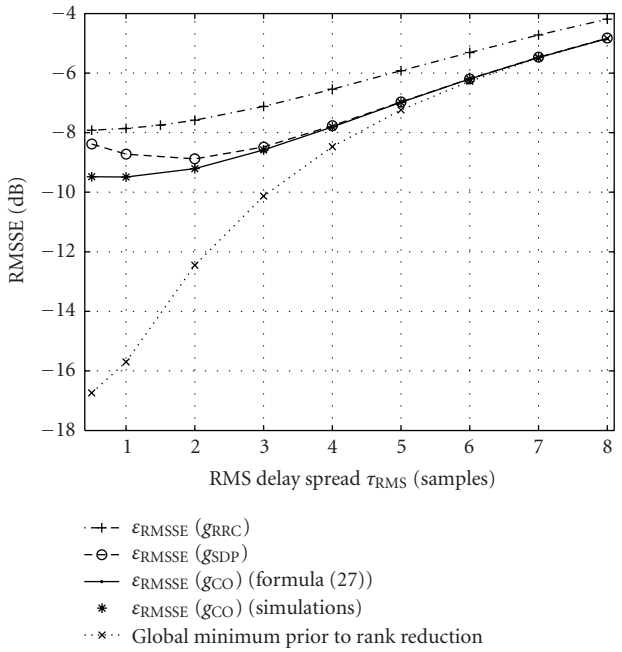

FIGURE 4: Model errors by windows $g_{\mathrm{CO}}[k]$ and $g_{\mathrm{SDP}}[k]$ optimized through CO and SDP, respectively, and by window $g_{\mathrm{RRC}}[k]$ with RRC-shaped magnitude spectrum versus τ_{RMS} at $\nu_{\mathrm{RMS}} = 10^{-2}$.

The generic matched filter sketched in Figure 5 aims to compute $u_1, \ldots, u_I$ in the TF domain. The TF representation R of the received signal $r[k]$ is obtained from an analysis filter bank, while TF representations $Z_1 \triangleq \mathcal{G}z_1, \ldots, Z_I \triangleq \mathcal{G}z_I$ of the elementary waveforms are provided by a local repository [32]. These are mapped to the TF representations $(H \odot Z_1), \ldots, (H \odot Z_I)$ of $(\mathcal{H}z_1)[k], \ldots, (\mathcal{H}z_I)[k]$ by means of the channel diagonalization (22) discussed in Section 4. Finally, taking advantage of Parseval's identity, $\hat{u}_i = \langle R, H \odot Z_i \rangle$ is computed for $i = 1, \ldots, I$.

The impact of the TF channel diagonalization on the ith matched filter output can be formulated as

$$\hat{u}_i - u_i = \langle R, H \odot Z_i \rangle - \langle r, \mathcal{H}z_i \rangle \tag{40}$$

$$= \langle R, \mathcal{G}\mathcal{G}^*(H \odot Z_i) \rangle - \langle r, \mathcal{H}z_i \rangle \tag{41}$$

$$= \langle r, \mathcal{G}^*(H \odot Z_i) \rangle - \langle r, \mathcal{H}z_i \rangle \tag{42}$$

$$= \langle r, \mathcal{G}^*(H \odot Z_i) - \mathcal{H}z_i \rangle = \langle r, e_i \rangle, \tag{43}$$

where for obtaining expression (41) we exploit that $R \in \mathcal{F}_g$ while $\mathcal{G}\mathcal{G}^*$ represents the orthogonal projection from $L^2(\Lambda)$ onto $\mathcal{F}_g$. The error signal $e_i[k] = (\mathcal{G}^*(H \odot \mathcal{G}z_i))[k] - (\mathcal{H}z_i)[k]$ is in line with the error signal definition (25). Under the assumptions that the relation between $\epsilon_Q[k]$ and $(\mathcal{H}x_Q)[k]$ found in Section 4 carries over to the relation between $e_i[k]$ and $(\mathcal{H}z_i)[k]$, and that $r[k]$ represents a random signal with $E[|\langle r, \mathcal{H}z_i \rangle|^2] = E[\|r\|^2]E[\|\mathcal{H}z_i\|^2]$ and $E[|\langle r, e_i \rangle|^2] = E[\|r\|^2]E[\|e_i\|^2]$, the RMSSE $\varepsilon_{\mathrm{RMSSE}}(g)$ determines the signal-to-noise ratio $E[|u_i|^2]/E[|\hat{u}_i - u_i|^2] = E[\|\mathcal{H}z_i\|^2]/E[\|e_i\|^2]$ at the matched filter output. Since the pulse $(\mathcal{H}z_i)[k]$ is typically a component of $r[k]$, the aforementioned assumptions, however, do not hold in general. Nevertheless, $\varepsilon_{\mathrm{RMSSE}}(g)$ may in practice serve as a rough characterization of the performance of the matched filter in Figure 5. The performance of the TF domain matched filtering in a reconfigurable receiver architecture configured to the reception of direct-sequence spread-spectrum signals is studied in [32].

8. Conclusions

We have derived paraunitary filter banks facilitating diagonalization of doubly dispersive channels at limited inherent MSE. Making use of a suitable parameterization of tight frames, we have shown that the optimization of paraunitary DFT filter banks for given channel statistics and oversampling factors can be formulated as a CO problem. An investigation of the MSE performance achieved by the optimized windows shows that the windows obtained by CO are more favorable than conventional windows with an RRC spectrum. However, in certain configurations the necessary rank reduction following the CO has a significant impact on the window shapes. The induced potential degradation of the MSE performance may be evaded by choosing appropriate lattice constants N and K, specifying the downsampling factor and the number of sub-bands, respectively, or by alternative rank reduction procedures which are yet to be devised. In general, the MSE performance can be improved at the cost of a higher complexity in terms of numbers of coefficients by increasing the oversampling factor.

In this paper our main concern was mathematical techniques for designing optimized filter banks in the context of channel diagonalization. Reconfigurable radios are clearly a prospective field of application. Since tight frames are natural generalizations of orthonormal bases used for the signal transform in OFDM receivers, the efficient handling of dispersive channels in OFDM can be inherited by receivers not limited to signals with cyclic extensions. Flexible radio architectures which incorporate the channel diagonalization considered in this paper have been investigated within the IST project URANUS (Universal RAdio-link platform for effieNt User-centric accesS) [34]. In this project the performance of such flexible receiver architectures has been studied in the context of different air interfaces and on different levels, from the inner receiver performance with perfect and imperfect channel estimation to the link level performance. While channel diagonalization by means of properly designed filter banks has been shown to have a great potential, there are a number of related issues that need to be addressed on the way to practical solutions, such as adequate channel estimation methods, synchronization, radio resource management, and others. A comparison of the performance of flexible receivers taking advantage of the channel diagonalization as compared to conventional receiver architectures has therefore been out of the scope of this paper.

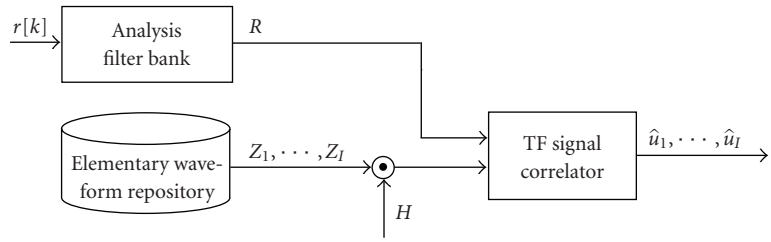

Figure 5: Generic TF domain matched filter.

Appendix

A. Derivation of RMSSE Formula

The RMSSE can be written as

$$\varepsilon_{\mathrm{RMSSE}}(g) = \varphi_1(g) + \varphi_2(g) - 2\varphi_3(g), \tag{A.1}$$

where

$$\varphi_1(g) \triangleq \lim_{Q\to\infty} E\left[\frac{1}{Q}\sum_{k=-Q/2}^{Q/2}\left|\sum_{(\ell,m)\in\Lambda} H[\ell,m]\langle x_Q, g_{\ell,m}\rangle g_{\ell,m}[k]\right|^2\right],$$
$$\varphi_2(g) \triangleq \lim_{Q\to\infty} E\left[\frac{1}{Q}\sum_{k=-Q/2}^{Q/2}\left|\sum_{q=0}^{\infty} c_{\mathcal{H}}[k,q]x_Q[k-q]\right|^2\right], \tag{A.2}$$

and

$$\varphi_3(g) \triangleq \lim_{Q\to\infty} E\left[\frac{1}{Q}\sum_{k=-Q/2}^{Q/2}\Re\left(\sum_{q=0}^{\infty}\sum_{(\ell,m)\in\Lambda} c_{\mathcal{H}}[k,q]x_Q[k-q] \times H^*[\ell,m]\langle x_Q, g_{\ell,m}\rangle^* g^*_{\ell,m}[k]\right)\right]. \tag{A.3}$$

Both the input signal power and the gain of the channel are normalized to unity, and therefore $\varphi_2 = 1$.

Furthermore, φ_1 can be expressed as

$$\varphi_1 = \lim_{Q\to\infty}\frac{1}{Q}\sum_{k=-Q/2}^{Q/2}\sum_{(\ell,m)\in\Lambda}\sum_{(\ell',m')\in\Lambda} E[H^*[\ell,m]H[\ell',m']] \times \sum_{k'=-Q/2}^{Q/2}\sum_{k''=-Q/2}^{Q/2} E\left[x_Q^*[k']x_Q[k'']\right] g_{\ell,m}[k']g^*_{\ell',m'}[k''] \times g^*_{\ell,m}[k]g_{\ell',m'}[k] \tag{A.4}$$

$$= \lim_{Q\to\infty}\frac{1}{Q}\sum_{k=-Q/2}^{Q/2}\sum_{(\ell,m)\in\Lambda}\sum_{(\ell',m')\in\Lambda}\sum_{q=0}^{\infty} \times \sum_{q'=0}^{\infty} E[c^*_{\mathcal{H}}[\ell N,q]c_{\mathcal{H}}[\ell' N,q']] \times e^{J2\pi(mq-m'q')/K} \times \sum_{k'=-Q/2}^{Q/2} g_{\ell,m}[k']g^*_{\ell',m'}[k']g^*_{\ell,m}[k]g_{\ell',m'}[k] \tag{A.5}$$

$$= \lim_{Q\to\infty}\frac{1}{Q}\sum_{(\ell,m)\in\Lambda_Q}\sum_{(\ell',m')\in\Lambda_Q}\phi_t[\ell' N-\ell N] \times \sum_{q=0}^{\infty} S_{\mathrm{delay}}[q]e^{J2\pi(m-m')q/K}\langle g_{\ell,m}, g_{\ell',m'}\rangle\langle g_{\ell',m'}, g_{\ell,m}\rangle, \tag{A.6}$$

where $\Lambda_Q = \{-\lfloor Q/2N\rfloor,\ldots,\lfloor Q/2N\rfloor\}\times\{0,\ldots,K-1\}$. To obtain (A.5) from (A.4) we apply (21), (20), and (24), and to arrive at (A.6) we use (18). Using (2) and (19), φ_1 can now be expressed as

$$\varphi_1 = \lim_{Q\to\infty}\frac{1}{Q}\frac{K}{N}\sum_{(\ell,m)\in\Lambda_Q}\phi_t[\ell N]\phi_f\left(\frac{2\pi m}{K}\right)\langle g_{\ell,m}, g_{0,0}\rangle\langle g_{0,0}, g_{\ell,m}\rangle = \frac{K}{N}\sum_{(\ell,m)\in\Lambda}\phi_t[\ell N]\phi_f\left(\frac{2\pi m}{K}\right)|\langle g_{0,0}, g_{\ell,m}\rangle|^2. \tag{A.7}$$

Finally φ_3 can be rewritten as

$$\varphi_3 = \lim_{Q\to\infty}\frac{1}{Q} \times \sum_{k=-Q/2}^{Q/2}\Re\left(E\left[\sum_{(\ell,m)\in\Lambda}\sum_{q=0}^{\infty} c_{\mathcal{H}}[k,q]\sum_{q'=0}^{\infty} c^*_{\mathcal{H}}[\ell N,q']e^{J2\pi mq'/k} \times g^*_{\ell,m}[k]\sum_{k'=-Q/2}^{Q/2} x_Q[k-q]x_Q^*[k']g_{\ell,m}[k']\right]\right) \tag{A.8}$$

$$= \lim_{Q\to\infty} \frac{1}{Q} \times \Re\left(\sum_{(\ell,m)\in\Lambda} \sum_{k=-Q/2}^{Q/2} \sum_{q=0}^{\infty} \sum_{q'=0}^{\infty} E[c_{\mathcal{H}}[k,q] c^*_{\mathcal{H}}[\ell N, q']] \times g^*_{\ell,m}[k] e^{\jmath 2\pi m q'/k} g_{\ell,m}[k-q] \right) \tag{A.9}$$

$$= \lim_{Q\to\infty} \frac{1}{Q} \times \Re\left(\sum_{(\ell,m)\in\Lambda_Q} \sum_{k=-Q/2}^{Q/2} \sum_{q=0}^{\infty} \phi_t[k-\ell N] \times S_{\text{delay}}[q] g^*_{\ell,m}[k] g_{\ell,m}[k-q] e^{\jmath 2\pi m q/k} \right) \tag{A.10}$$

$$= \lim_{Q\to\infty} \frac{1}{Q} \frac{K}{N} \Re\left(\sum_{k=-Q/2}^{Q/2} \phi_t[k] \sum_{q=0}^{\infty} S_{\text{delay}}[q] g_{0,0}[k-q] g^*_{0,0}[k] \right) \tag{A.11}$$

$$= \frac{K}{N} \Re\Big(\Big\langle \Big(g_{0,0} * S_{\text{delay}} \Big) \odot \phi_t, g_{0,0} \Big\rangle \Big). \tag{A.12}$$

We use (24) to obtain (A.9) from (A.8), and for the derivation of (A.10), (18) is applied. Thus, the RMSSE is given by

$$\varepsilon_{\text{RMSSE}}(g) = 1 + \frac{K}{N} \left(\sum_{(\ell,m)\in\Lambda} \phi_t[\ell N] \phi_f\left(\frac{2\pi m}{K}\right) |\langle g, g_{\ell,m}\rangle|^2 - 2\Re\Big(\Big\langle \Big(g * S_{\text{delay}} \Big) \odot \phi_t, g \Big\rangle \Big) \right). \tag{A.13}$$

References

[1] H. Sari, G. Karam, and I. Jeanclaude, "Frequency-domain equalization of mobile radio and terrestrial broadcast channels," in *Proceedings of IEEE Global Telecommunications Conference (GLOBECOM '94)*, pp. 1–5, San Francisco, Calif, USA, November 1994.

[2] D. Falconer, S. L. Ariyavisitakul, A. Benyamin-Seeyar, and B. Eidson, "Frequency domain equalization for single-carrier broadband wireless systems," *IEEE Communications Magazine*, vol. 40, no. 4, pp. 58–66, 2002.

[3] I. Martoyo, *Frequency domain equalization in CDMA detection*, Ph.D. thesis, Institut für Nachrichtentechnik, University of Karlsruhe, 1995.

[4] F. Adachi, A. Nakajima, K. Takeda, et al., "Frequency-domain equalisation for block CDMA transmission," *European Transactions on Telecommunications*, vol. 19, no. 5, pp. 553–560, 2008.

[5] H. Bölcskei and F. Hlawatsch, "Discrete zak transforms polyphase transforms and applications," *IEEE Transactions on Signal Processing*, vol. 45, no. 4, pp. 851–866, 1997.

[6] Z. Ju, T. Hunziker, and D. Dahlhaus, "Time-frequency parameterization of doubly dispersive channels," in *Proceedings of the European Signal Processing Conference (EUSIPCO '09)*, Glasgow, UK, August 2009.

[7] P. P. Vaidyanathan, *Multirate Systems and Filter Banks*, Prentice-Hall, Englewood Cliffs, NJ, USA, 1993.

[8] P. Jung and G. Wunder, "The WSSUS pulse design problem in multicarrier transmission," *IEEE Transactions on Communications*, vol. 55, no. 10, pp. 1918–1928, 2007.

[9] S.-M. Phoong, Y. Chang, and C.-Y. Chen, "DFT-modulated filterbank transceivers for multipath fading channels," *IEEE Transactions on Signal Processing*, vol. 53, no. 1, pp. 182–192, 2005.

[10] P. Jung and G. Wunder, "Iterative pulse shaping for Gabor signaling in WSSUS channels," in *Proceedings of IEEE Workshop on Signal Processing Advances in Wireless Communications (SPAWC '04)*, pp. 368–372, Lisbon, Portugal, 2004.

[11] P. Schniter, "A new approach to multicarrier pulse design for doubly-dispersive channels," in *Proceedings of the Allerton Conference on Communication, Control, and Computing*, Monticello, Ill, USA, October 2003.

[12] T. Strohmer and S. Beaver, "Optimal OFDM design for time-frequency dispersive channels," *IEEE Transactions on Communications*, vol. 51, no. 7, pp. 1111–1122, 2003.

[13] M. G. Bellanger, "Specification and design of a prototype filter for filter bank based multicarrier transmission," in *Proceedings of IEEE International Conference on Acoustics, Speech, and Signal Processing (ICASSP '01)*, vol. 4, pp. 2417–2420, 2001.

[14] W. Kozek and A. F. Molisch, "Nonorthogonal pulseshapes for multicarrier communications in doubly dispersive channels," *IEEE Journal on Selected Areas in Communications*, vol. 16, no. 8, pp. 1579–1589, 1998.

[15] S. Houwen, T. Chen, and S. A. Norman, "Design of FIR multirate filter banks using convex optimization," in *Proceedings of IEEE Pacific RIM Conference on Communications, Computers, and Signal Processing*, vol. 1, pp. 469–472, Victoria, Canada, August 1997.

[16] J. Xu and T. Strohmer, "Pulse construction in OFDM systems via convex optimization," *IEEE Transactions on Communications*, vol. 56, no. 8, pp. 1225–1230, 2008.

[17] B. Borna and T. N. Davidson, "Efficient filter bank design for filtered multitone modulation," in *Proceedings of IEEE International Conference on Communications*, vol. 1, pp. 38–42, Paris, France, June 2004.

[18] M. R. Wilbur, T. N. Davidson, and J. P. Reilly, "Efficient design of oversampled NPR GDFT filterbanks," *IEEE Transactions on Signal Processing*, vol. 52, no. 7, pp. 1947–1963, 2004.

[19] H. H. Kha, H. D. Tuan, and T. Q. Nguyen, "Efficient design of cosine-modulated filter banks via convex optimization," *IEEE Transactions on Signal Processing*, vol. 57, no. 3, pp. 966–976, 2009.

[20] A. Karmakar, A. Kumar, and R. K. Patney, "Design of an optimal two-channel orthogonal filterbank using semidefinite programming," *IEEE Signal Processing Letters*, vol. 14, no. 10, pp. 692–694, 2007.

[21] H. Bölcskei, F. Hlawatsch, and H. G. Feichtinger, "Equivalence of DFT filter banks and Gabor expansions," in *Wavelet Applications in Signal and Image Processing III*, vol. 2569 of *Proceedings of SPIE*, pp. 128–139, San Diego, Calif, USA, July 1995.

[22] Z. Cvetkovic and M. Vetterli, "Tight Weyl-Heisenberg frames in $\ell^2(\mathbb{Z})$," *IEEE Transactions on Signal Processing*, vol. 46, no. 5, pp. 1256–1259, 1998.

[23] H. G. Feichtinger and T. Strohmer, *Gabor Analysis and Algorithms: Theory and Applications*, Birkhäuser, Boston, Mass, USA, 1998.

[24] K. Gröchenig, *Foundations of Time-Frequency Analysis*, Birkhäuser, Boston, Mass, USA, 2001.

[25] J. Kovačević and A. Chebira, "Life beyond bases: the advent of frames (Part I)," *IEEE Signal Processing Magazine*, vol. 24, no. 4, pp. 86–104, 2007.

[26] J. Kovačević and A. Chebira, "Life beyond bases: the advent of frames (Part II)," *IEEE Signal Processing Magazine*, vol. 24, no. 5, pp. 115–125, 2007.

[27] H. G. Feichtinger, M. Hampejs, and G. Kracher, "Approximation of matrices by Gabor multipliers," *IEEE Signal Processing Letters*, vol. 11, no. 11, pp. 883–886, 2004.

[28] S. Boyd and L. Vandenberghe, *Convex Optimization*, Cambridge University Press, Cambridge, UK, 2004.

[29] G. H. Golub and C. F. V. Loan, *Matrix Computations*, Johns Hopkins University Press, Baltimore, Md, USA, 3rd edition, 1996.

[30] A. J. E. M. Janssen and P. L. Søndergaard, "Iterative algorithms to approximate canonical Gabor windows: computational aspects," *Journal of Fourier Analysis and Applications*, vol. 13, no. 2, pp. 211–241, 2007.

[31] P. A. Bello, "Characterization of randomly time-variant linear channels," *IEEE Transactions on Communications Systems*, vol. 11, pp. 360–393, 1963.

[32] T. Hunziker, Z. Ju, and D. Dahlhaus, "A reconfigurable baseband receiver architecture based on time-frequency signal processing," in *Proceedings of the ICT Mobile and Wireless Communications Summit*, Santander, Spain, June 2009.

[33] T. Hunziker and S. Stefanatos, "Efficient two-dimensional filters for doubly-dispersive channel estimation in time-frequency signal processing," in *Proceedings of the 10th IEEE International Symposium on Spread Spectrum Techniques and Applications (ISSSTA '08)*, pp. 381–385, Bologna, Italy, August 2008.

[34] European research project IST-27960, URANUS (Universal RAdio-link platform for efficieNt User-centric accesS), http://www.ist-uranus.org/.